Suggesting double-web I-shaped columns for omitting continuity plates in a box-shaped column

Hamed Saffari [*1], Amir A. Hedayat [2b] and Nasrin Soltani Goharrizi [3c]

[1] *Department of Civil Engineering, Shahid Bahonar University of Kerman, Kerman, Iran*
[2] *Department of Civil Engineering, Kerman Branch, Islamic Azad University, Kerman, Iran*
[3] *Department of Civil Engineering, Yazd Branch, Islamic Azad University, Yazd, Iran*

Abstract. Generally the required strength and stiffness of an I-shaped beam to the box-shaped column connection is achieved if continuity plates are welded to the column flanges from all sides. However, welding the forth edge of a continuity plate to the column flange may not be easily done and is normally accompanied by remarkable difficulties. This study was aimed to propose an alternative for box columns with continuity plates to diminish such problems. For this purpose a double-web I-shaped column was proposed. In this case the strength and rotational stiffness of the connection was provided by nearing the column webs to each other. Finite element studies on about 120 beam-column connections showed that the optimum proportion of the distance between two column webs and the width of the column flange (parameter β) was a function of the ratio of the beam flange width to the column flange width (parameter α). Hence, based on the finite element results, an equation was proposed to estimate the optimum value of parameter β in terms of parameter α to achieve the highest connection performance. Results also showed that the strength and ductility of post-Northridge connections of such columns are in average 12.5 % and 54% respectively higher than those of box-shaped columns with ordinary continuity plates. Therefore, a double-web I-shaped column of optimum arrangement might be a proper replacement for a box column with continuity plates when beams are rigidly attached to it.

Keywords: strength; ductility; moment resisting connections; box columns; continuity plates

1. Introduction

In the 1994 Northridge earthquake, brittle fractures in beam-column connection areas occurred causing considerable damage. These damages depend on the specifications of its main components, namely the columns, beams and connections. Following this event, various related institutions have been conducting experimental researches on the behavior of steel beam- column connection. Based on these researches there are only two sources to dissipate seismic energy, the beam-end and the panel zone Engelhardt and Sabol (1998), Saffari *et al*. (2013), Farrokhi *et al*. (2010). AISC specification ANSI/AISC (2010) presents some flange and web strength requirements for columns

---

when they are subjected to double concentrated forces (one tensile and one compressive) delivered to column flanges through welded and bolted moment connections. These requirements are needed to prevent some limit states such as flange local bending, web local yielding, web crippling and web compression buckling. In the case of using columns of inadequate strength for their flanges and webs, such limit states can be prevented by welding transverse stiffeners to the column flanges and webs at the level of beam flanges. These stiffeners are also called continuity plates. These plates also help to distribute beam flange forces to the column web, and they minimize stress concentrations that can occur in the joint between the beam flange and the column due to non-uniform stiffness of the column flange. Hence, for both I-shaped and box-shaped columns, the use of continuity plates as thick as the beam flange plates has been emphasized by FEMA-355D (2000) to provide good seismic performance for beam-to-column connections. Large flexural and torsional stiffness and high strength of any axes of box-shaped columns make these sections more efficient than conventional wide flange I-shaped sections. These caused a box-shaped column to be more attractive for designers than an I-shaped column when being used as a beam-column. Although box-columns have these advantages, as the section is closed, welding of the forth side of the continuity plate to the column is not easily done. In addition to the above problems, the welders may frequently forget to perform this plate in the column and if so, welding the plate inside the column won't be possible anymore. Hence, finding a proper beam to column connection to diminish such problems is still an interesting subject for researchers. Up to now different types of external stiffeners, including triangular plates, T- and angle-stiffeners have been proposed by researchers to provide a proper load path between the I-beam and the rolled box-column Shanmugam *et al*. (1991), Ting *et al*. (1993), Lee and Yoon (1993), Popov (1987). Recently, for built-up box-shaped columns, some new connection details called diagonal through-plate connection have been proposed by Mirghaderi *et al*. (2010) and Torabian *et al*. (2012) to eliminate the horizontal continuity plates. However, their details are relatively complicated and may not be easily fabricated.

In the present study to eliminate the use of continuity plates in the built-up box-shaped columns and consequently to facilitate their fabrication and to supply adequate torsional stiffness for I-shaped columns, double-web I-shaped columns are suggested. Using finite element method, a parametric study was done to find out the best configuration of such columns to achieve adequate connection strength and stiffness.

2. Proposed double-web I-column

In Iran a common design for low to middle rise steel buildings is to use moment frames in one direction while braced frames are used in the other. Based on this common design and with respect
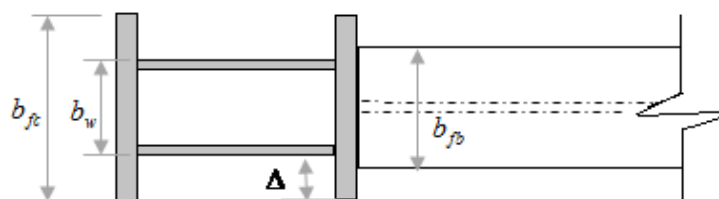

Fig. 1 The proposed double-web I-shaped column

to the fact that box-shaped columns have a high flexural-torsional buckling strength, Fig. 1 shows the details for the proposed double-web I-shaped column where a beam is rigidly attached to the column only in one direction. In fact, this column is a built-up box-shaped where the web plates have moved toward the column center to form an I-box column. In this case the continuity plates are removed and the stiffness and strength of the connection is supplied through nearing the webs of the box-shaped column to an optimal distance.

3. Finite element model

In this study the finite element modeling can be categorized into two parts. The first part is about widened flange specimen W08-L1A, a pre-tested specimen by Cheng *et al*. (2006), which was used for the validation of the finite element modeling. The second part is about B-SAC and B-SPE specimens which were used for parametric studies. This section explains the common points between the two parts and the details of the W08-L1A specimen. B-SAC and B-SPE specimens are discussed in the following section.

Finite element models were created using the general purpose finite element program ANSYS (ANSYS user manual 2007). In finite element models, both welds and base metals were modeled using shell elements, and the associated material property was defined for each one. SHELL43 was used to model weld and column plates, whereas SHELL181 was used to model the beam plates. SHELL43 and SHELL181 are one-layer four-node and multi-layer eight-node shell elements respectively. These elements have six degrees of freedom at each node, and all of them have plasticity, large deflection, and large strain capabilities. In the case of using SHELL181, each element was separated into five layers across the thickness. The number of layers was selected based on the finite element study carried out by Gilton and Uang (2002). To perform material nonlinearity analyses, plasticity behavior was based on the von-Mises yielding criteria and the associated flow rule. Isotropic hardening was assumed for the monotonic analysis, whereas kinematic hardening was assumed for the cyclic analysis as used by Mao *et al*. (2001) and Ricles *et al*. (2003). A bilinear material response with a post yielding stiffness equal to 4% of the modulus of elasticity of steel was used for the base metals, whilst for the weld metals; a multi-linear material response (Fig. 2) based on material property given in the references of Mao *et al*. (2001) and Ricles *et al*. (2003) was used.
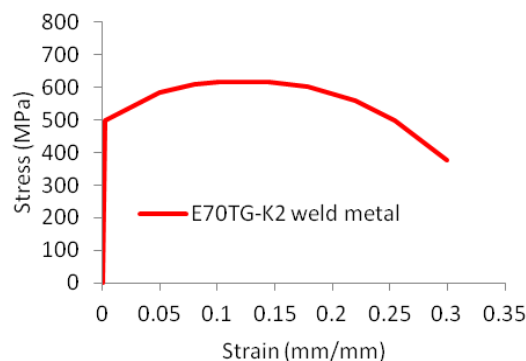

Fig. 2 Stress-strain relationship used for the weld metal (Mao *et al*. 2001, Ricles *et al*. 2003)
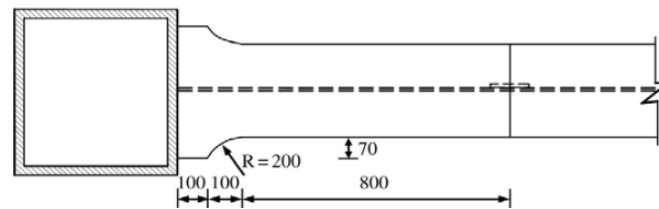
Fig. 3 box-shaped column to I-shaped beam connection W08L1A tested by Cheng *et al*. (2006)

The monotonic analyses were conducted by applying a monotonic vertical displacement load to the beam tip until achieving more than 4% total rotation at the column web center, whereas the load history recommended in reference FEMA350 (2000) was utilized for cyclic analyses. In order to determine the appropriate mesh density, a study on mesh sensitivity was carried out based on the recommendation given by ANSYS software and then the results were compared with the experimental results presented by Cheng *et al*. (2006). When applied loads are in the vertical direction only, the out-of-plane deformations (normal to the web) may not occur. Therefore, in order to ensure that buckling occurs when the model becomes unstable, the imperfect model was used to analyze under cyclic or monotonic loadings. In this study, in order to determine the imperfect model, first the buckling mode shapes were computed in a separate buckling analysis, and then they were implemented to perturb the original perfect geometry of the model as it was in References of Hedayat and Celikag 2009b, c, Kim *et al*. (2000), MoslehiTabar and Deylami, (2005).

As mentioned above, in order to verify the accuracy of the finite element modeling, the pretested box-shaped column to I-shaped beam connection, specimen W08-L1A of reference Cheng *et al*. (2006) (see Fig. 3), was modeled using the procedure mentioned in the previous paragraphs. In this connection, the widened beam flange was intended to reinforce the beam-to-column joint and form the plastic hinge away from the column face. Fig. 4 shows the finite element mesh of this specimen and Fig. 5 depicts the welding details for the specimen without the weld access hole detail. As this figure shows the beam flanges were double bevel groove welded to the column flange. As mentioned above these groove welds were modeled using the SHELL elements with a total width of 10 mm (the average of 13 mm and 7 mm), and a material property similar to what is shown in Fig. 2 (i.e.., weld metal E70TG-K2) was assigned for the welds. For simplicity, the fillet welds which connect the beam flange to the beam web were not modeled since they would not affect the results.

The W08-L1A specimen consisted of an H-shaped H588 × 300 × 12 × 20 (dimensions in mm for depth, width, web thickness, and flange thickness, respectively) beam, 3030 mm long and a box column of 550 × 550 × 27 × 27 with 3000 mm span length. The thicknesses of the continuity plates were the same as those of the beam flange plates (i.e., 20 mm). The beam, the column and the continuity plates were all ASTM A572 Grade 50 steel. Constraints of this specimen were consistent with the test set-up (i.e., one end of the column was considered as a pin support, a roller support was assigned to the other end of the column, and the beam was laterally braced at its tip and near the location of the splices of the beam flanges and web). This specimen consisted of 14,880 nodes and 9100 elements. As shown in Fig. 4, from the mesh size point of view, the beam length was divided into three parts. A very fine mesh size was used for the welds at the column face level and for the beam flanges located at the vicinity of the column face (mesh size was 10 mm).
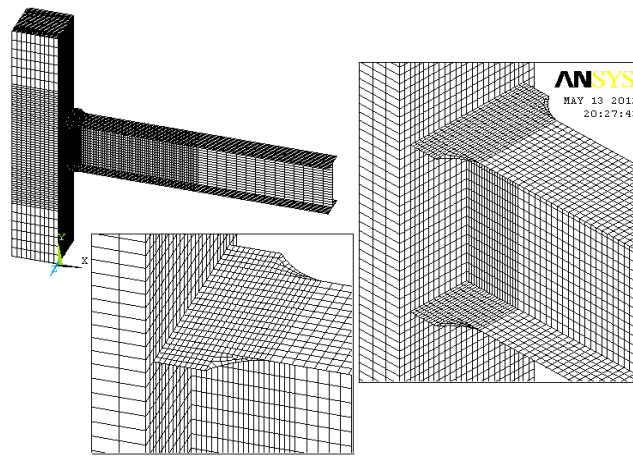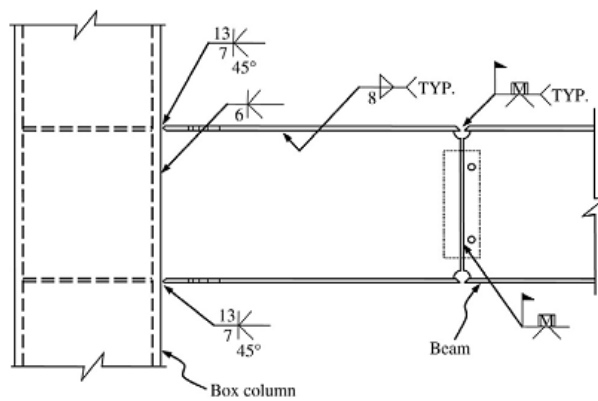
Fig. 4 Finite element mesh of specimen W08L1A

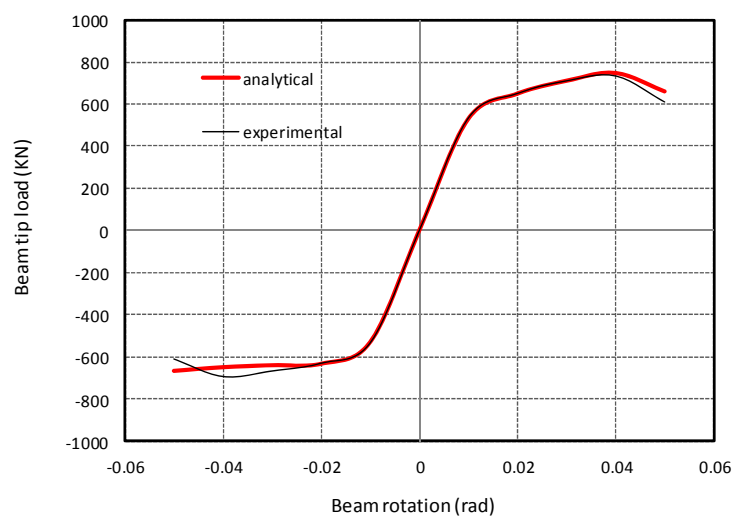Fig. 5 Welding details of specimen W08-L1A tested by Cheng *et al*. (2006)

Fig. 6 Comparison between analytical and experimental results of specimen W08L1A

By moving from the column face toward the beam tip, the mesh sizes gradually increased. The mesh size used for the second part of the beam was 20 mm and for the third part of the beam, where the elements are away enough from the column face level and the plastic hinge location, the size was 60 mm.

Experimental and numerical results of this specimen were compared in terms of beam tip load and beam rotation. Fig. 6 shows this comparison. The initial stiffness, maximum load achieved at the peak of the beam tip displacement and post-elastic envelopes under upward loadings were well matched for the finite element model and the test specimen. However, when the loads became downward a minor mismatch could be seen between the two curves at large rotations. Therefore, it might be concluded that the analytical results are in good agreement with experimental results.

4. Parametric study

In this study all parametric studies were done for B-SAC and B-SPE group specimens which represent a wide range of connections of different beam overall depths (from 450 mm to 912 mm). Details of these specimens are presented in Table 1. B-SAC and B-SPE specimens comprised of a built-up box-shaped column and a rolled wide flange I-shaped beam. The beams used for B-SPE specimens had a thicker flange compared to those of B-SAC specimens. The reason of using B-SPE specimens was due to this fact that for a given beam overall depth, by increasing the beam flange thickness, the connection ductility reduces. The connection details of all specimens were exactly the same as the SAC and the SPE specimens presented by Lee *et al*. (2000) and Hedayat *et al*. (2009b) respectively. It means all specimens had post-Northridge connection detail except that the box-shaped columns were used instead of I-shaped columns. For instance, Fig. 7 shows the details of the specimen SAC7 utilized by Lee *et al*. (2000). The length of the beam and the column for all these specimens were 3429 mm and 3658 mm respectively. Other geometric parameters of these specimens are summarized in Table 2. Both the shear tab and continuity plates were ASTM A36 (yield stress = 250 MPa), and all welds were E70TG-K2 electrode.

After Northridge earthquake, inspections done by Miller (1998) over 100 damaged buildings and also experimental tests conducted by the SAC group (e.g., Lee *et al*. 2000) on the pre and the post-Northridge connections showed that the failure of this type of connection is not often due to the failure of bolts. Therefore, in the finite element models, the bolts were not exactly modeled, but the shear tab and the bolt holes were modeled. In addition, the interaction between the shear tab and the beam web was modeled using the CONTACT elements in the ANSYS program. For the SAC and the SPE specimens, by using the long and the thick shear plates and adequate number of slip critical bolts which connect the shear tab to the beam web, there was no slippage between the shear tab and the beam web even at the failure time (as it was obvious from the moment-rotation curves presented by Lee *et al*. 2000). Hence, to simplify the finite element models and to connect the beam web to the shear tab, by using couple command in the ANSYS program, for each bolt hole the translational degrees of freedom of all nodes around the holes in the shear tab and in the beam web were constrained together. The finite elements' results of SAC specimens obtained using this procedure of bolt modeling were in good agreements with those of experimental results presented by Lee *et al*. (2000). This comparison can be found in the literature Hedayat *et al*. (2009b).

Similar to the W08-L1A specimen, from the mesh size point of view, the beam length was divided into three parts. For the first part of the beam which started from the column face and ended at a distance equal to the half of the beam overall depth, a very fine mesh size was used for

the welds and for the beam flanges (depending on the beam section, mesh size varied between 3 mm and 5 mm; weld size was divided into five elements along the beam length). For the second part of the beam whose length was 1.5 times of the beam overall depth, the mesh sizes were larger than those used at the column face level, and they varied between 15 mm and 25 mm. The used mesh sizes for the third part of the beam, where the elements are enough away from the column face level, were in average equal to 80 mm.

Box-shaped columns were designed as such to have exactly the same capacity as that of I-shaped columns used in SAC and SPE specimens presented in the related references. All the designs were developed using ANSI/AISC (2010) specification ANSI/AISC (2010). These specimen sizes were chosen since they might be good representatives of the conventional pre/post Northridge specimen sizes, small, medium and large Lee *et al.* (2000), and were also tested in Phase 1 of SAC Steel Projects SAC-96-01 (1996).

The effects of nearing the webs of a box-shaped column (Fig. 1) on the strength, ductility and stiffness of a post-Northridge connection were investigated using parameters $\alpha = b_{fb} / b_{fc}$ and $\beta = b_w / b_{fb}$ where $b_w = b_{fc} - 2\Delta$ and b_{fb}, b_w, b_{fc} and Δ are shown in Fig. 1. Parameter β varied between zero (which represent an ordinary I-shaped column) and a value greater than one (which represent an ordinary box-shaped column). This parametric study was done to determine the most proper placement of the column webs to achieve the highest connection performance. In addition to these, the results of each B-SAC and B-SPE specimen for a given value of parameter β were compared to those of the same specimen with a detail similar to what are shown in Fig. 8 for specimens B0 to B3. In specimen B0, continuity plates are welded to all sides of a box column. While for specimens B1 to B3, continuity plates are welded to the column flange and web plates only from three sides.

Table 1 Details of B-SPE and B-SAC groups

| Specimen	Type	Section/Size (mm)	Yield stress (MPa)
B-SAC7	Beam	W36*150	250
	Column	BOX-420*400*45*25	345
B-SPE7	Beam	W36*170	250
	Column	BOX-420*400*45*25	345
B-SAC5	Beam	W30*99	250
	Column	BOX-405*405*30*15	345
B-SPE5	Beam	W30*116	250
	Column	BOX-405*405*30*15	345
B-SAC3	Beam	W24*68	250
	Column	BOX-375*375*20*10	345
B-SPE3	Beam	W24*84	250
	Column	BOX-375*375*20*10	345
B-SPE2	Beam	W18*55	250
	Column	BOX-305*305*20*10	345
B-SPE1	Beam	W18*46	250
	Column	BOX-305*305*20*10	345
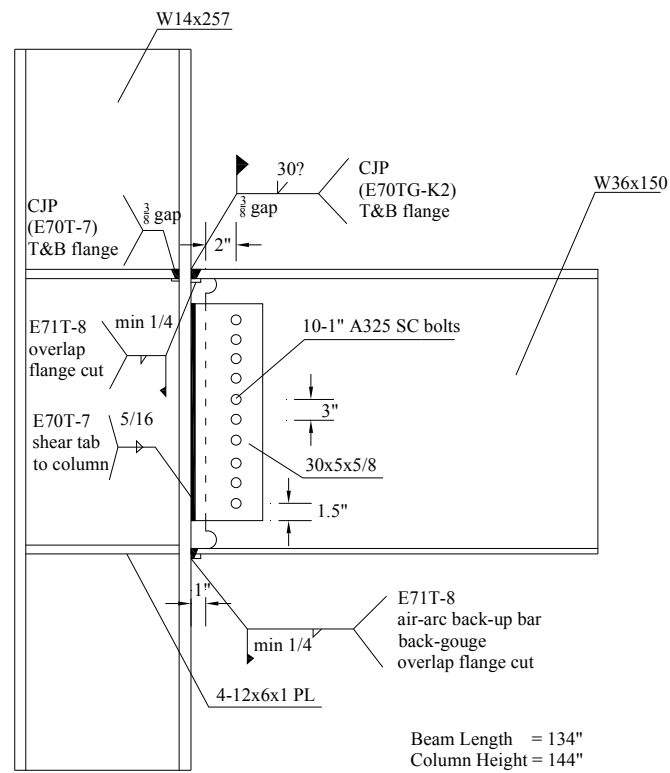
Fig. 7 Specimen SAC7 utilized by Lee *et al*. (2000)
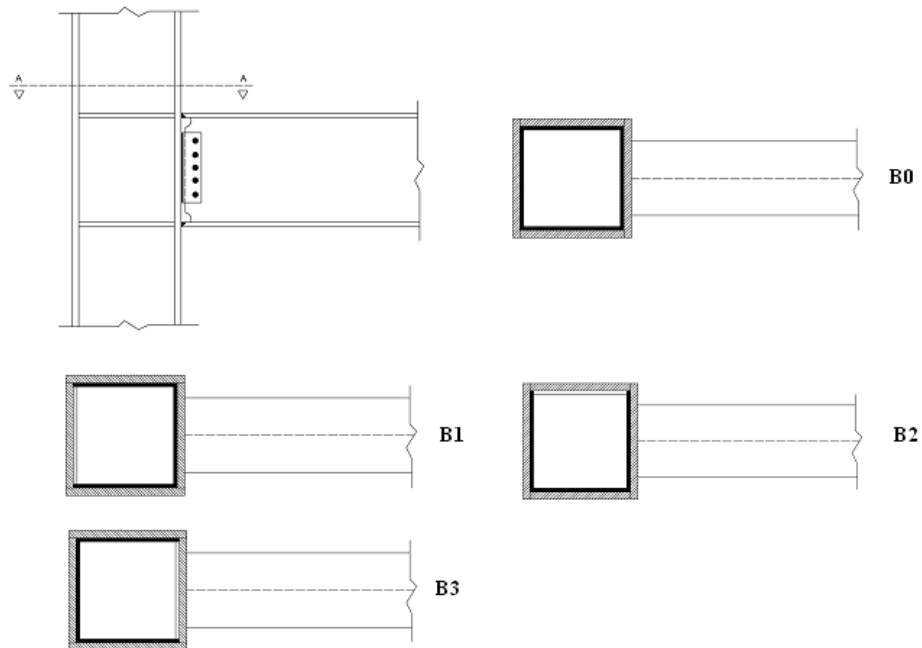
Fig. 8 Specimens B0 to B3, representing different situations of continuity plate connection to the beam

Table 2 Geometric parameters of SAC and SPE specimens

Specimen	Shear tab (mm)	No. of A325 SC Bolts (mm)	Continuity plate (mm)	Weld type and size (mm)	
				Beam flange	shear tab
SPE1	324x127x10.32	4Φ22	285x265x16	CJP, root opening = 9 mm, bevel angle = 30° and E70TG-K2	Fillet, 8 mm, E70T-7
SPE2	324x127x10.32	4Φ22	285x265x16		Fillet, 8 mm, E70T-8
SAC3	457x127x9.50	6Φ22	355x335x16		Fillet, 8 mm, E70T-7
SPE3	457x127x11.91	6Φ25	355x335x19		Fillet, 8 mm, E70T-8
SAC5	610x127x12.70	8Φ25	375x345x19		Fillet, 8 mm, E70T-7
SPE5	610x127x14.29	8Φ29	375x345x22		Fillet, 8 mm, E70T-7
SAC7	762x127x15.88	10Φ25	350x330x25		Fillet, 8 mm, E70T-7
SPE7	762x127x17.47	10Φ29	350x330x29		Fillet, 8 mm, E70T-8

5. Analytical results

5.1 Typical behavior of a post-Northridge connection with a double-web I-shaped column

5.1.1 Failure criteria and failure modes

It should be noted that fracture prediction is the most questionable part of a finite element study, because it is inherently a complicated phenomenon and is dependent on many parameters such as weld and base metal properties, weld defects, notch effects, weld quality and weld toughness. Hence, in this study in order to estimate the connection failure time, it was assumed that the qualified welders and fabricators are employed, and high fracture toughness weld metals are used (as these should be, based on ANSI/AISC (2010)). Also, it is well known that in the welded connections at a region near the column face the classic beam theory is invalid Hedayat and Celikag 2009a, Kim *et al*. (2000), Lee and Yoon (1999), Cheol (2006). In this region, shear stresses are at a maximum level near the column flanges, especially at the WAH region. The combination of shear stresses and normal stresses at the beam flanges near the column face, promotes the brittle fracture of welded connections. Therefore, the use of von-Mises strains might be more appropriate than normal strains to estimate the failure of material near the column face and even at a region away from the column face. Considering the fact that the locations of high level of strains have significant probability of premature fractures and by comparing the results of finite element models of SAC specimens with their experimental results presented by Lee *et al*. (2000), a failure criterion was assumed as follows:

Connection fracture occurs when von-Mises strains at the half or entire beam or column flange widths (depends on connection type) at the column face level exceed the stain associated with the ultimate strength of the beam or column flange materials, based on the material properties reported by Lee *et al*. (2000). These failure modes are shown in Fig. 9. However, to ensure the estimation of the connection failure time, in some models, Birth and Death characteristics of elements in ANSYS software were also used.

A similar failure criterion was also used by other researchers (e.g., Berman *et al*. (2010); Dusicka *et al*. (2004)). Note that the connection failure can also be predicted using rupture index, RI (e.g., Chao *et al*. (2006), Prinz and Richards (2009)). But this method is normally used when a

(a) (b)
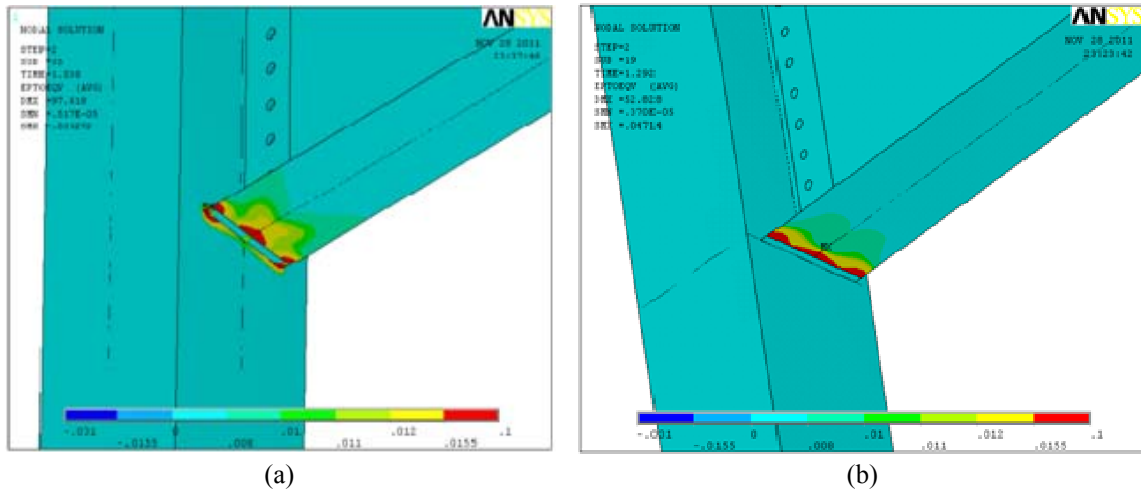
Fig. 9 Fracture of connection: (a) at column flange; (b) at beam flange

reduction is made in the beam section especially within the web area. However, as stated by most of researchers (e.g., Prinz and Richards (2009)), none of the mentioned methods is intended to predict the exact rotation capacities for connections; rather, they provide a tool for comparing various models.

5.1.2 Von-Misses strain distribution across the beam flange width

Fig. 10 shows the normalized Von-Misses strain distribution for specimens B-SAC7 in the case of using an ordinary box-shaped column (specimen B0) and a double-web I-shaped column of β = 0.41 at 2 percent total rotation. Results are compared at 2 percent total rotation since normally non-modified post-Northridge connections (i.e., a specimen without flange plates, haunches or

Fig. 10 Normalized Von-Misses strain distribution for whole beam flange width at the weld access hole region at 2 percent total rotation

reduced beam section, RBS) have such a rotational capacity. Total rotation was measured at the column web center. Normalized strains were obtained at the most critical location of a post-Northridge connection, weld access hole (WAH) region, by dividing the measured Von-Mises strain by the yield strain of the beam flange material. As indica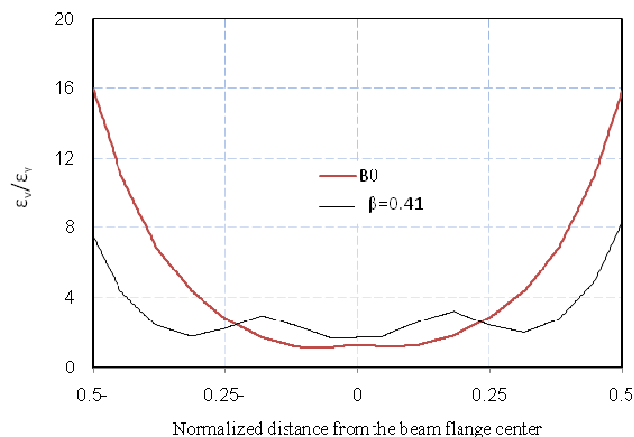ted in the figure, the level of strains at the beam flange edges are much more than those which were measured at the beam flange center, indicating that the connection fracture initiates from the beam flange edge. This figure also shows that at the critical locations (i.e., beam flange edges) the level of the developed strains for the proposed double-web I-shaped column is less than half of that measured for the specimen B0. It indicates that the proposed column section was significantly effective to minimize the stress and the strain concentrations at the joint which was due to the presence of double column webs to create a more uniform stiffness of the column flange across its width. This significant reduction in the strain concentration caused the post-Northridge connections of the proposed column section to show higher connection strength and ductility than those of B0 specimens. Similar behaviors were also observed for all other SAC and SPE specimens. Strength and ductility of all specimens are discussed in the following sections.

5.1.3 Effects of the proposed double-web I-shaped column on the secondary flexural stresses

FEMA-355D (2000) states that in box-shaped columns even in the presence of continuity plates, the beam web connection is consistently less effective in transferring bending moment and beam shear to the box-shaped column than it is for strong-axis column-bending connections. As a result, many of the benefits through enhanced web connections for the welded-flange-welded-web and free-flange connections are not readily achieved with box-shaped column connections. As a result, the connection type does not rely heavily on the web connection for its connection ductility. Fig. 11 shows the distribution of normal strains at the outer surface of the bottom beam flange along the beam length at 2 percent total rotation for B-SAC7 specimens.

Normal strains and the distance from the column face were normalized with respect to the yield strain of the beam flange material and the beam overall depth respectively. These distributions are
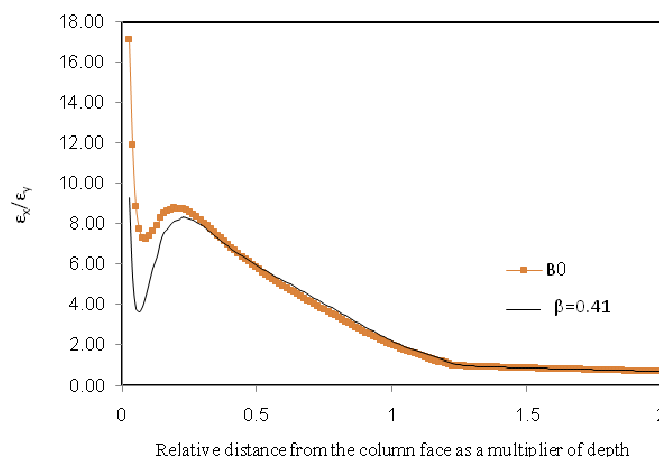

Fig. 11 Normalized distribution of normal strains for B-SAC7 specimens B0 and double-web
I-shaped column of $\beta = 0.41$ at the beam flange edge at 2 percent total rotation

presented at the beam flange edge (i.e., at the critical location of a box column) for specimens B-SAC7 in the case of using an ordinary box-shaped column (specimen B0) and a double-web I-shaped column of $\beta = 0.41$. As this figure shows for both specimens the distribution of normalized strains is linear and follows the classical beam theory beyond about 15 percent of the beam overall depth from the column face. However, at the column face, normalized strains suddenly increased. This increase was due to the secondary flexural stresses which were resulted from the transfer of a remarkable part of shear forces via the beam flanges (which is in contrast with the classical beam theory). This figure clearly shows the efficiency of the proposed double-web I-shaped column to reduce the normal strains at the column face level. Compared with specimen B0, there was a 46 percent reduction in the amount of the normal strains at the peak of the diagram when the double-web I-shaped column specimen of $\beta = 0.41$ was used. It indicates a remarkable improvement in transferring the bending moment and beam shear to the box-shaped column via the web connection. It consequently caused an increase in the connection strength and ductility.

5.1.4 Effects of the proposed double-web I-shaped column on the connection strength, ductility and initial rotational stiffness

Fig. 12 compares the moment-rotation curves for all B-SPE7 specimens. In this figure total rotations were calculated at the column web center, and the applied moments were calculated at the column face and were normalized with respect to the beam plastic moment capacity. As this figure shows, among all specimens, the double-web I-shaped column specimen of $\beta = 1.37$ (i.e., a box-shaped column without continuity plates) has the minimum connection strength, ductility and initial rotational stiffness. The maximum strength of this specimen was only 80 percent of the beam plastic moment. This connection failed due to the excessive strain concentration at the column flange (a failure mode similar to Fig. 9(a)). By a decrease in parameter β all connection strength, ductility and initial rotational stiffness increased. The highest connection performance was achieved for specimen of $\beta = 0.41$. Also this figure shows that specimens B0 and B1 have the
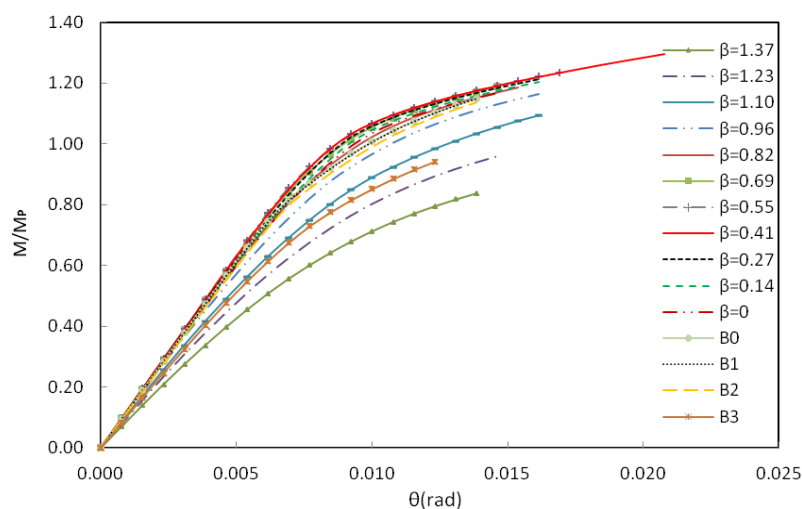

Fig. 12 Moment-rotation curves for all B-SPE7 specimens

same performance, while there can be seen a slight reduction in the performance of specimen B2 when compared with specimens B0 and B1.As it was expected specimen B3 achieved a low connection strength, ductility and initial rotational stiffness. Its performance was somehow similar to double-web specimen of $\beta = 1.23$ with a lower ductility.

5.2 The results and summary of specimen

Table 3 summarizes strength, ductility and normalized initial rotational stiffness of all B-SAC and B-SPE specimens in terms of parameter β. For comparison, the strength and ductility of all B0 to B3 specimens are also presented. In this table total rotations were calculated at the column web center, and failure moments were normalized with respect to the beam plastic moment in each specimen. As the results show, for both B-SAC and B-SPE specimens, by decreasing β parameter both connection strength and ductility increases. However, excessive increase in this parameter causes a reduction in both connection strength and ductility. In other words, there is an optimum value for parameter β to achieve the highest connection strength and ductility. These optimum specimens are highlighted in Table 3.

Compared to using a box-shaped column with ordinary continuity plates, the use of a double-web I-shaped column of optimum value of parameter β caused minimum 43% and maximum 65.5% (in average 54%) increase in the connection ductility while the minimum and the maximum enhancement in the connection strength were 9% and 16% respectively (in average 12.5%). It indicates that the proposed column was more effective to enhance the connection ductility rather than the connection strength. However, all double-web I-shaped columns of

Table 3 Finite element results of all B-SAC and B-SPE specimens

Specimen type	Beam section	Column section	α	β	Total rotation θ (%)	Failure moment, M (kN.m)	M/MP	Normalized initial rotational stiffness
				Specimen				
B-SAC7	W 36*150	BOX420*400*45*25	0.76	1.37	1.62	2363.13	0.99	0.76
				1.23	1.54	2558.00	1.07	0.84
				1.10	1.46	2704.04	1.14	0.92
				0.96	1.38	2786.31	1.17	0.98
				0.82	1.46	2899.43	1.22	1.01
				0.69	1.54	2968.75	1.25	1.03
				0.55	1.77	3084.90	1.3	1.03
				0.41	**2.08**	**3211.26**	**1.35**	**1.03**
				0.27	1.54	2958.90	1.24	1.01
				0.14	1.46	2900.79	1.22	1.00
				0.00	1.46	2889.14	1.21	0.99
				B0	1.46	2882.41	1.21	1.00
				B1	1.46	2878.33	1.21	0.99
				B2	1.46	2805.01	1.18	0.95
				B3	1.46	2599.50	1.09	0.88

Specimen type	Beam section	Column section	α	β Specimen	Total rotation θ (%)	Failure moment, M (kN.m)	M/MP	Normalized initial rotational stiffness
B-SPE7	W 36*170	BOX420*400*45*25	0.763	1.37	1.38	2294.52	0.84	0.74
				1.23	1.46	2621.73	0.96	0.82
				1.10	1.62	2992.96	1.09	0.90
				0.96	1.62	3186.19	1.16	0.97
				0.82	1.54	3246.36	1.19	1.00
				0.69	1.46	3249.83	1.19	1.02
				0.55	1.69	3381.47	1.24	1.03
				0.41	**2.08**	**3542.74**	**1.29**	**1.02**
				0.27	1.62	3321.10	1.21	1.01
				0.14	1.62	3293.53	1.20	0.99
				0.00	1.46	3195.45	1.17	0.98
				B0	1.38	3146.84	1.15	1.00
				B1	1.38	3140.32	1.15	0.99
				B2	1.38	3114.50	1.14	0.97
				B3	1.23	2579.79	0.94	0.87
B-SAC5	W 30*99	BOX405*405*30*15	0.655	1.52	1.62	751.40	0.59	0.51
				1.37	1.62	888.18	0.69	0.63
				1.22	1.69	1073.91	0.84	0.75
				1.07	1.69	1287.45	1.01	0.89
				0.91	1.46	1351.00	1.06	0.96
				0.76	1.38	1429.30	1.12	1.00
B-SAC5	W 30*99	BOX405*405*30*15		0.61	1.54	1515.02	1.19	1.02
			BOX405*405*30*15	**0.46**	**2.23**	**1651.01**	**1.29**	**1.02**
				0.3	1.69	1541.82	1.21	1.01
				0.15	1.38	1446.81	1.13	0.99
				0.00	1.31	1412.51	1.11	0.98
				B0	1.38	1415.17	1.11	1.00
				B1	1.38	1409.21	1.10	0.99
				B2	1.38	1373.97	1.07	0.94
				B3	1.31	910.47	0.71	0.71
B-SPE5	W 30*116	BOX405*405*30*15	0.66	1.52	1.38	744.74	0.48	0.50
				1.37	1.31	871.45	0.56	0.61
				1.22	1.31	1054.41	0.68	0.74
				1.07	1.38	1330.56	0.86	0.88
				0.91	1.54	1583.20	1.02	0.95

Specimen type	Beam section	Column section	α	β	Total rotation θ (%)	Failure moment, M (kN.m)	M/MP	Normalized initial rotational stiffness
				Specimen				
B-SPE5	W 30*116	BOX405*405*30*15	0.66	0.76	1.62	1718.94	1.11	0.98
				0.61	1.69	1771.69	1.14	1.00
				0.46	**2.38**	**1905.75**	**1.23**	**1.00**
				0.30	1.85	1791.23	1.16	0.99
				0.15	1.62	1713.57	1.11	0.96
				0.00	1.31	1597.13	1.03	0.95
				B0	1.46	1731.35	1.12	1.00
				B1	1.46	1728.15	1.12	0.99
				B2	1.46	1669.39	1.08	0.94
				B3	1.08	903.06	0.58	0.69
B-SAC3	W 24*68	BOX375*375*20*10	0.607	1.64	1.77	310.95	0.43	0.38
				1.47	1.62	361.97	0.50	0.49
				1.31	1.46	427.66	0.59	0.63
				1.14	1.46	532.01	0.73	0.79
				0.98	1.54	675.51	0.93	0.93
				0.82	1.85	821.90	1.13	0.99
				0.65	1.92	872.10	1.20	1.01
				0.49	**2.31**	**920.75**	**1.27**	**1.02**
				0.33	1.54	822.78	1.13	1.01
				0.16	1.23	736.57	1.02	0.98
				0.00	1.23	724.33	1.00	0.97
				B0	1.54	798.75	1.10	1.00
				B1	1.54	797.62	1.10	0.99
				B2	1.54	769.98	1.06	0.93
				B3	1.23	377.18	0.52	0.60
B-SPE3	W 24*84	BOX375*375*20*10	0.61	1.64	1.54	308.40	0.34	0.35
				1.47	1.38	361.18	0.39	0.46
				1.31	1.31	442.37	0.48	0.60
				1.14	1.23	548.12	0.60	0.77
				0.98	1.38	748.29	0.81	0.9
				0.82	1.62	946.44	1.03	0.96
				0.65	2.00	1076.72	1.17	0.98
				0.49	**2.31**	**1122.29**	**1.22**	**0.99**
				0.33	1.15	1054.74	1.85	0.97
				0.16	1.31	909.99	0.99	0.95
				0.00	1.23	846.29	0.92	0.94

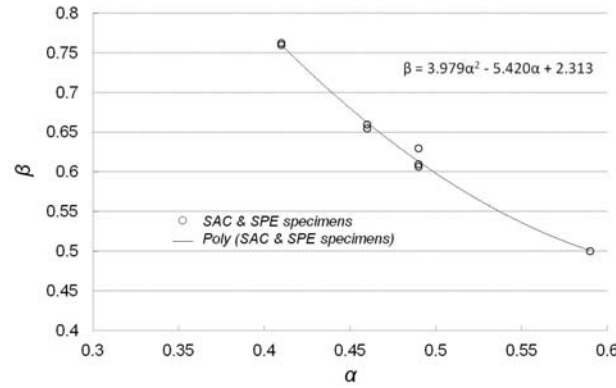| Specimen type	Beam section	Column section	α	β	Total rotation θ (%)	Failure moment, M (kN.m)	M/MP	Normalized initial rotational stiffness
				Specimen				
B-SPE3	W 24*84	BOX375*375*20*10		B0	1.62	1023.43	1.12	1.00
				B1	1.62	1022.15	1.11	0.99
				B2	1.69	993.49	1.08	0.93
				B3	1.08	380.58	0.41	0.57
B-SPE2	W 18*55	BOX305*305*20*10	0.63	1.63	1.85	204.54	0.45	0.46
				1.47	1.77	241.57	0.53	0.57
				1.31	1.69	290.04	0.63	0.70
				1.14	1.69	355.37	0.77	0.83
				0.98	1.92	454.28	0.99	0.93
				0.82	2.08	511.35	1.11	0.97
				0.53	2.77	557.14	1.21	0.99
				0.49	**3.31**	**579.10**	**1.26**	**0.99**
				0.33	2.54	543.02	1.18	0.98
				0.16	1.77	489.70	1.07	0.96
				0.00	1.69	470.37	1.03	0.95
				B0	2.00	524.02	1.14	1.00
				B1	2.00	523.39	1.14	0.99
				B2	2.00	507.78	1.11	0.94
				B3	1.31	237.80	0.52	0.66
B-SPE1	W 18*46	BOX305*305*20*10	0.50	1.98	1.85	163.26	0.44	0.40
				1.78	1.69	181.63	0.49	0.48
				1.58	1.62	210.61	0.57	0.58
				1.39	1.62	251.78	0.68	0.70
				1.19	1.69	307.48	0.83	0.83
				0.99	2.00	380.10	1.02	0.95
				0.79	2.15	414.16	1.11	1.01
				0.59	**2.54**	**437.95**	**1.18**	**1.02**
				0.40	2.31	427.57	1.15	1.02
				0.20	2.08	413.03	1.11	1.00
				0.00	2.00	406.52	1.09	0.99
				B0	1.69	379.60	1.02	1.00
				B1	1.69	378.99	1.02	0.99
				B2	1.69	370.41	1.00	0.94
				B3	1.31	190.74	0.51	0.60

Fig. 13 Relation between parameter α and optimum value of parameter β for all SPE and SAC specimens

optimum value of parameter β easily achieved a connection strength more than the minimum required strength (i.e., $M/Mp = 0.8$).

To see the effect of each proposed alternative on the connection initial rotational stiffness, these values were normalized with respect to the initial rotational stiffness of specimen B0. This ratio for all double-web I-shaped column specimens of optimum value of parameter β (those highlighted in Table 3) was around 1.01. It indicates that a connection with a double-web I-shaped column of optimum value of parameter β has an initial rotational stiffness the same as that for a specimen with a box-shaped column with ordinary continuity plates. However, the fabrication of the proposed column is much easier when it is compared to a box-shaped column where the continuity plates should be welded from all sides to the column flanges.

As it is clear from the results presented in Table 3, the optimum value of parameter β is not a constant value and changes from one specimen to another. For instance, for B-SAC7 specimens (where $\alpha = 0.76$) the optimum value of parameter β was 0.41 while for B-SPE1 specimens (where $\alpha = 0.5$) the highest connection performance was achieved at $\beta = 0.56$. In fact, this optimum value is a function of parameter α, where α is the beam flange width to the column flange width ratio. The relation between optimum values of parameter β and parameter α are graphically shown in Fig. 13. As the figure shows by increasing parameter α, the optimum value of parameter β decreased. With respect to these results, an equation was proposed to estimate the optimum value of parameter β in terms of parameter α (Eq. (1)).

$$\beta = 3.979\alpha^2 - 5.42\alpha + 2.313 \tag{1}$$

6. Conclusions

Generally the required strength and stiffness of an I-shaped beam to a box-shaped column connection is achieved if continuity plates are welded to the column flanges from all sides. However, welding the forth edge of a continuity plate to the column flange may not be easily done and is normally accompanied with a remarkable difficulties. This study was aimed to propose an alternative for box columns with continuity plates to diminish such problems. For this purpose a double-web I-shaped column was proposed. In this case the strength and rotational stiffness of the

connection was provided by nearing the column webs to each other. To find out the optimum distance between the two column webs, a parametric study was done on about 120 specimens of beams of different depths and sections.

Finite element results showed that the optimum proportion of the distance between the two column webs and the width of the column flange (parameter β) is not a constant value and is a function of the beam flange width to the column flange width ratio (parameter α). Hence, based on the finite element results, an equation was proposed to estimate the optimum value of parameter β in terms of parameter α to achieve the highest connection performance. This relationship is presented by Eq. (1) in the text. Results also showed that the proposed column section was significantly effective to minimize the stress and the strain concentrations at the joint. Such a positive effect was due to the presence of the double column webs to create a more uniform stiffness of the column flange across its width. In addition, results indicated a remarkable improvement in the transferring of the bending moment and the beam shear to the box-shaped column via web connection. It consequently caused an increase in the connection strength and ductility. Strength and ductility of a post-Northridge connection of a double-web I-shaped column of optimum value of parameter β were in average 12.5 % and 54% respectively higher than those of a box-shaped column with ordinary continuity plates. Also these connections had initial rotational stiffness the same as those for rigid connections with box-shaped columns with continuity plates.

Specimens of the optimum column section (a double-web I-shaped column of optimum value of parameter β) could easily achieve the minimum required connection strength. Despite the remarkable enhancement in the connection ductility in the presence of a double-web I-shaped column, still the rotational capacity of these modified specimens is less than the minimum required ductility (total rotation = 4 percent). Hence, as stated by FEMA-355D, to achieve the minimum required connection ductility, the beam end configuration of such specimens must be modified by employing either the weakening of the beam section method (e.g., RBS connections) or strengthening of the connection (e.g., using cover plates or haunches). In addition, with this method there is no need for continuity plates with their remarkable fabrication difficulties. Therefore, a double-web I-shaped column of optimum value of parameter β might be a proper replacement for a box-shaped column with continuity plates when beams are rigidly attached to it.

References

ANSI/AISC 360-10 (2010), "Specification for structural steel buildings", American Institute of Steel Construction.

ANSYS user manual (2007), ANSYS, Inc.

Berman, J.W., Okazaki, T. and Hauksdottir, H.O. (2010), "Reduced link sections for improving the ductility of eccentrically braced frame link-to-column connections", *J. Struct. Eng.*, **136**(5), 543-553.

Chao, S.H., Khandelwal, K. and El-Tawil, S. (2006), "Ductile web fracture initiation in steel shear links", *J. Struct. Eng.*, **132**(8), 1192-1200.

Cheng, C.C., Chun, C.L. and Chieh, H.L. (2006), "Ductile moment connections used in steel column-tree moment-resisting frames", *J. Constr. Steel Res.*, **62**(8), 793-801.

Cheol, H.L. (2006), "Review of force transfer mechanism of welded steel moment connections", *J. Constr. Steel Res.*, **62**(7), 695-705.

Dusicka, P., Itani, A.M. and Buckle, L.G. (2004), "Finite element investigation of steel built-up shear links subjected to inelastic deformations", *Earthquake Eng. Struc.*, **3**(2), 195-203.

Engelhardt, M.D. and Sabol, T.A. (1998), "Reinforcing of steel moment connections with cover plates:

Benefits and modifications", *J. Eng. Struct.*, **20**(4-6), 510-520.

Farrokhi, H., Ahmadi, D.F. and Eshghi, S. (2010), "The on structural detailing effect seismic behavior of steel moment resisting connections", *Struct. Eng. Mech., Int. J.*, **35**(5), 617-630.

FEMA350 (2000), "Recommended seismic design criteria for new steel moment-frame buildings", Washington D.C., Federal Emergency Management Agency.

FEMA-355D (2000), "State of the art report on connection performance", Washington D.C., Federal Emergency Management Agency.

Gilton, C.S. and Uang, C.M. (2002), "Cyclic response and design recommendations of weak-axis reduced beam section moment connections", *J. Struct. Eng.*, **128**(4), 452-463.

Hedayat, A.A. and Celikag, M. (2009a), "Fracture moment and ductility of welded connection", *Proceeding of the Institution of Civil Engineers - Structures and Buildings*, UK, December, **162**(6), 405-418.

Hedayat, A.A. and Celikag, M. (2009b), "Post-Northridge connection with modified beam end configuration to enhance strength ductility", *J. Constr. Steel Res.*, **65**(7), 1413-1430.

Hedayat, A.A. and Celikag, M. (2009c), "Wedge design: A reduced beam web (RBW) connection for seismic regions", *Adv. Struct. Eng.*, **13**(2), 263-290.

Kim, T., Whittaker, A.S., Gilani, A.S., Bertero, V.V. and Takhirov, S.M. (2000), "Cover-Plate and Flange-Plate reinforced steel-moment resisting connections", SAC/BD-00/27.

Lee, C.H. and Yoon, T.H. (1999), "Analytical re-examination of shear transfer in welded steel moment connection", *Proceeding of the 1st Japan-Korea Joint Seminar on Earthquake Engineering for Building Structures*, Seoul, Korea, October, **1**, 119-128.

Lee, H., Stojadinovic, B., Goel, S.C., Margarian, A.G., Choi, J. and Wongkaew, A. (2000), *Parametric Tests on Unreinforced Connections*, SAC/BD-00/01, Volume I – Final Report.

Lee, S.L., Ting, L.C. and Shanmugam, N.E. (1993), "Use of external T-stiffeners in box-column to I-beam connections", *J. Constr. Steel Res.*, **26**(2-3), 77-98.

Mao, C., Ricles, J., Lu, L. and Fisher, J. (2001), "Effect of local details on ductility of welded moment connections", *J. Struct. Eng.*, **127**(9), 1036-1044.

Miller, D.K. (1998), "Lessons learned from the Northridge earthquake", *Eng. Struct.*, **20**(4-6), 249-260.

Mirghaderi, S.R., Torabian, S. and Keshavarzi, F. (2010), "I-beam to box-column connection by a vertical plate passing through the column", *Eng. Struct.*, **32**(8), 2034-2048.

MoslehiTabar, A. and Deylami, A. (2005), "Instability of beams with reduced beam section moment connections emphasizing the effect of column panel zone ductility", *J. Constr. Steel Res.*, **6**(11), 1475-1491.

Popov, E.P. (1987), "Panel zone flexibility in seismic moment joints", *J. Constr. Steel Res.*, **8**, 91-118.

Prinz, G.S. and Richards, P.W. (2009), "Eccentrically braced frame links with reduced web sections", *J. Constr. Steel Res.*, **65**(10-11), 1971-1978.

Ricles, J.M., Mao, C., Lu, L.W. and Fisher, J.W. (2003), "Ductile details for welded unreinforced moment connections subject to inelastic cyclic loading", *Eng. Struct.*, **25**(5), 667-680.

SAC-96-01 (1996), "Experimental investigations of beam-column subassemblies", Report No. SAC-96-01, SAC Joint Venture, Sacramento, CA, USA.

Saffari, H., Hedayat A.A. and Poorsadeghi Nejad, M. (2013), "Post-Northridge connections with slit dampers to enhance strength and ductility", *J. Constr. Steel Res.*, **80**, 138-152.

Shanmugam, N.E., Ting, L.C. and Lee, S.L. (1991), "Behaviour of I-beam to box-column connections stiffened externally and subjected to fluctuating loads", *J. Constr. Steel Res.*, **20**(2), 129-148.

Stojadinović, B., Goel, S., Lee, K., Margarian, A. and Choi, J. (2000), *Parametric Tests on Unreinforced Connections*, SAC/BD-00/01, Vol. I: Final Report.

Ting, L.C., Shanmugam, N.E. and Lee, S.L. (1993), "Design of I-beam to box-column connections stiffened externally", *Eng. J.*, **30**(4), 141-149.

Torabian, S., Mirghaderi, S.R. and Keshavarzi, F. (2012), "Moment-connection between I-beam and built-up square column by a diagonal through plate", *J. Constr. Steel Res.*, **70**, 385-401.

CC